

Spin partners of the $Z_b(10610)$ and $Z_b(10650)$ revisited

V. Baru^{a,b} E. Epelbaum^a A. A. Filin^a C. Hanhart^c A. V. Nefediev^{b,d,e}

^a*Institut für Theoretische Physik II, Ruhr-Universität Bochum, D-44780 Bochum, Germany*

^b*Institute for Theoretical and Experimental Physics, B. Chermushkinskaya 25, 117218 Moscow, Russia*

^c*Forschungszentrum Jülich, Institute for Advanced Simulation, Institut für Kernphysik and Jülich Center for Hadron Physics, D-52425 Jülich, Germany*

^d*National Research Nuclear University MEPhI, 115409, Kashirskoe highway 31, Moscow, Russia*

^e*Moscow Institute of Physics and Technology, 141700, Institutsky lane 9, Dolgoprudny, Moscow Region, Russia*

E-mail: vadimb@tp2.rub.de, evgeny.epelbaum@ruhr-uni-bochum.de,
arseniy.filin@ruhr-uni-bochum.de, c.hanhart@fz-juelich.de,
nefediev@itep.ru

ABSTRACT: We study the implications of the heavy-quark spin symmetry for the possible spin partners of the exotic states $Z_b(10610)$ and $Z_b(10650)$ in the spectrum of bottomonium. We formulate and solve numerically the coupled-channel equations for the Z_b states that allow for a dynamical generation of these states as hadronic molecules. The force includes short-range contact terms and the one-pion exchange potential, both treated fully nonperturbatively. The strength of the potential at leading order is fixed completely by the pole positions of the Z_b states so that the mass and the most prominent contributions to the width of the isovector heavy-quark spin partner states W_{bJ} with the quantum numbers J^{++} ($J = 0, 1, 2$) come out as predictions. In particular, we predict the existence of an isovector 2^{++} tensor state lying a few MeV below the $B^*\bar{B}^*$ threshold which should be detectable in the experiment. Since the accuracy of the present experimental data does not allow one to fix the pole positions of the Z_b 's reliably enough, we also study the pole trajectories of their spin partner states as functions of the Z_b binding energies. It is shown that, once the heavy-quark spin symmetry is broken by the physical B and B^* mass difference, especially the pion tensor force has a significant impact on the location of the partner states clearly demonstrating the need of a coupled-channel treatment of pion dynamics to understand the spin multiplet pattern of hadronic molecules.

KEYWORDS: exotic hadrons, bottomonium, chiral dynamics, effective field theory

Contents

1	Introduction	1
2	Contact theory	5
3	One-pion exchange interaction	7
4	Results and discussion	10
4.1	Dependence on the HQSS breaking scale	10
4.2	Dependence on the one-boson-exchange strength parameter	11
4.3	Dependence on the input for the Z_b 's binding energies	12
5	Comment on the pionless theory	15
6	Conclusions	16

1 Introduction

The experimental discovery of the charmonium-like state $X(3872)$ by the Belle Collaboration in 2003 [1] inaugurated a new era in hadron spectroscopy. A lot of new candidates for exotic states have been discovered since then in the spectrum of both charmonium and bottomonium — for a review see, for example, Refs. [2, 3]. Among those one should especially mention the isovector $Z_b(10610)$ and $Z_b(10650)$ resonances (for brevity, hereinafter often referred to as Z_b and Z'_b , respectively) [4–6]. Their signals are seen in 7 channels, namely

$$\begin{aligned}\Upsilon(10860) &\rightarrow \pi Z_b^{(\prime)} \rightarrow \pi B^{(*)} \bar{B}^*, \\ \Upsilon(10860) &\rightarrow \pi Z_b^{(\prime)} \rightarrow \pi\pi\Upsilon(nS), \quad n = 1, 2, 3, \\ \Upsilon(10860) &\rightarrow \pi Z_b^{(\prime)} \rightarrow \pi\pi h_b(mP), \quad m = 1, 2.\end{aligned}\tag{1.1}$$

Since Z_b and Z'_b are charged but decay into final states containing a b and an anti- b quark they must contain at least four quarks and are thus explicitly exotic. It turned out that the decays of the Z_b 's into the open-flavour channels almost exhaust their widths, despite the limited phase spaces. This feature is to be regarded as a strong evidence for a molecular nature of the Z_b states [7] — for a recent review of the theory of hadronic molecules we refer to Ref. [8].

The corresponding masses and widths extracted from the Breit-Wigner fits for the data and averaged over the above production and decay channels are [9]

$$M_{Z_b} = 10607.2 \pm 2.0 \text{ MeV}, \quad \Gamma_{Z_b} = 18.4 \pm 2.4 \text{ MeV},\tag{1.2}$$

$$M_{Z'_b} = 10652.2 \pm 1.5 \text{ MeV}, \quad \Gamma_{Z'_b} = 11.5 \pm 2.2 \text{ MeV},\tag{1.3}$$

to be compared with 10604 MeV and 10649 MeV for the $B\bar{B}^*$ and the $B^*\bar{B}^*$ thresholds, respectively. Therefore, both poles are located within a couple of MeV from the respective threshold. The J^{PC} quantum numbers of both states were determined as 1^{+-} [10] in line with the expectation of the molecular model.

Within the molecular picture, the wave functions of the Z_b states can be written as [7]

$$1^+(1^{+-}) : |Z_b\rangle = -\frac{1}{\sqrt{2}} \left[(1_{b\bar{b}}^- \otimes 0_{q\bar{q}}^-)_{S=1} + (0_{b\bar{b}}^- \otimes 1_{q\bar{q}}^-)_{S=1} \right], \quad (1.4)$$

$$1^+(1^{+-}) : |Z'_b\rangle = \frac{1}{\sqrt{2}} \left[(1_{b\bar{b}}^- \otimes 0_{q\bar{q}}^-)_{S=1} - (0_{b\bar{b}}^- \otimes 1_{q\bar{q}}^-)_{S=1} \right], \quad (1.5)$$

where we quote the quantum numbers in the form $I^G(J^{PC})$ and, for example, $1_{b\bar{b}}^-$ denotes the wave function of the $b\bar{b}$ pair with the total spin 1, and so forth. Such an identification of the Z_b 's allows one to explain the dipion transition rates from the $\Upsilon(10860)$ to the vector bottomonia $\Upsilon(nS)$ ($n = 1, 2, 3$), which appear to be up to two orders of magnitude larger than similar transitions among the lower bottomonia $\Upsilon(nS)$ ($n = 1, 2, 3$) [11]. In addition, the molecular interpretation of the Z_b 's (see Eqs. (1.4)-(1.5)) naturally explains that transitions such as $Z_b^{(\prime)} \rightarrow \pi h_b(mP)$, which are expected to be suppressed by $(\Lambda_{\text{QCD}}/m_b)$ since they involve a change in the heavy-quark spin, happen at a comparable rate to the heavy-quark spin preserving transitions $Z_b^{(\prime)} \rightarrow \pi\Upsilon(nS)$ [4].

Molecular states should in general be located below the most relevant threshold and not above¹, which seems to be in conflict with the numbers quoted in Eqs. (1.2) and (1.3). However, these numbers need to be interpreted with care. While they show unambiguously that the poles related to the Z_b states reside very close to the corresponding open-flavour thresholds, their particular values contain an uncontrollable intrinsic systematic uncertainty since they were determined from sums of the Breit-Wigner functions that ignore the nearby thresholds and which, therefore, appear to be in conflict with analyticity and unitarity. Also, it is argued, for example, in Ref. [14] (see also Ref. [15] for a related discussion in the context of $f_0(980)/a_0(980)$) that the branching fractions extracted from the Breit-Wigner parameterisations do not represent the decay probabilities for near-threshold states. Thus, a more refined data analysis is required. For example, it is demonstrated in Ref. [16] that both Z_b 's are compatible with bound state poles in the data for the $h_b(mP)\pi$ channels as soon as the energy dependence of their self-energies is included properly. On the other hand, a combined analysis of the experimental data in all seven channels listed in Eqs. (1.1) consistent with analyticity and unitarity favours both Z_b 's as virtual states located within approximately 1 MeV below the respective thresholds [17, 18]². In other words, the quality of the existing data does not allow one to draw definite conclusions about the pole locations of these states. Thus, in the present paper, we investigate the fate of the symmetry partners of the Z_b states as the binding energies of the latter are

¹Meson-meson dynamics can also lead to above-threshold poles if the interaction is energy-dependent, but such states are not expected to be very narrow [12]. On the other hand, a tetraquark nature of the states is claimed to result in the poles lying slightly above threshold [13].

²While the formalism of these references is indeed unitary with respect to all seven channels, only the open-flavour and the $h_b(mP)\pi$ channels were included in the fit, since the $\Upsilon(nS)\pi$ channels call for an additional inclusion of nonresonant production.

varied up to zero. As soon as the analysis of Refs. [17, 18] is refined to include one-pion exchange interactions, the predictions for the partner states would have become possible directly from the fit for the experimental line shapes. However, a detailed investigation of the line shapes, which also calls for an inclusion of the inelastic channels, is delegated to future studies.

In the limit of an infinite b -quark mass, a molecular nature of the Z_b states allows one to predict the existence of spin partners with the quantum numbers $J^{PC} = J^{++}$, conventionally denoted in the literature as W_{bJ} , with $J = 0, 1, 2$ [7, 19, 20] (see also Ref. [21] for a recent review and for the discussion of the future experimental tasks). In particular, in the notations of Eqs. (1.4) and (1.5), the wave functions of the spin partners take the form

$$1^-(0^{++}) : |W_{b0}\rangle = \frac{1}{2} \left[\sqrt{3}(1_{b\bar{b}} \otimes 1_{q\bar{q}})_{S=0} - (0_{b\bar{b}} \otimes 0_{q\bar{q}})_{S=0} \right], \quad (1.6)$$

$$1^-(0^{++}) : |W'_{b0}\rangle = \frac{1}{2} \left[(1_{b\bar{b}} \otimes 1_{q\bar{q}})_{S=0} + \sqrt{3}(0_{b\bar{b}} \otimes 0_{q\bar{q}})_{S=0} \right], \quad (1.7)$$

$$1^-(1^{++}) : |W_{b1}\rangle = (1_{b\bar{b}} \otimes 1_{q\bar{q}})_{S=1}, \quad (1.8)$$

$$1^-(2^{++}) : |W_{b2}\rangle = (1_{b\bar{b}} \otimes 1_{q\bar{q}})_{S=2}. \quad (1.9)$$

Although a detailed microscopic theory is needed to predict individual decay widths of the Z_b and W_{bJ} states, the spin symmetry allows one to arrive at various relations between their total widths, for example [19],

$$\Gamma[Z_b] = \Gamma[Z'_b], \quad (1.10)$$

$$\Gamma[W_{b1}] = \Gamma[W_{b2}] = \frac{3}{2}\Gamma[W_{b0}] - \frac{1}{2}\Gamma[W'_{b0}], \quad (1.11)$$

and [20]

$$\Gamma[Z_b] = \Gamma[Z'_b] = \frac{1}{2} (\Gamma[W_{b0}] + \Gamma[W'_{b0}]). \quad (1.12)$$

Additional predictions for the partial decay widths into various hidden-bottom final states can be also found in Refs. [19, 20].

To arrive at the above predictions the mass splitting

$$\delta = m_* - m = 45 \text{ MeV} \quad (1.13)$$

was treated as a large scale (compared to the binding energies) which was integrated out. Hereinafter m and m_* denote the B and B^* masses, respectively. While this assumption is acceptable for the Z_b states themselves³, for their spin partner it turns out to be appropriate only within a truncated scheme when only the S -wave interactions are retained. However, it is the central finding of this paper that, as soon as the one-pion exchange (OPE) is included, the effect of the mass difference δ is enhanced significantly via the strong S - D transitions that come with it. This results in binding energies of the spin partner states as

³The first correction to the leading-order result (1.12) is controlled by the parameter $\sqrt{E_B/\delta}$ [22], which, for example, for the binding energy $E_B = 5$ MeV yields the uncertainty around 30%.

large as 20 MeV, which are clearly of the order of the spin symmetry violating parameter δ — see Eq. (1.13). While pion exchanges were already included in studies of the Z_b states before [23], to the best of our knowledge its impact on the spin partners has not been investigated so far. Furthermore, since, in Ref. [24], the effect of the OPE was claimed to be somewhat diminished if the one- η exchange (OEE) is added, we also investigate the effect of this addition.

It is well known that a nonperturbative inclusion of the OPE interaction in the chiral nuclear effective-field theory allows one to significantly extend the region of applicability of the theory — see, for example, Refs [25, 26]. In charmonium-like systems such as the $X(3872)$, pionic effects turn out to be important to predict the dynamical properties such as the light-quark mass dependence of the X -pole [27, 28] (for a discussion of the pion mass dependence with perturbative pions we refer to Ref. [29]) and the decay width $X(3872) \rightarrow D\bar{D}\pi$ [30]. Furthermore, it was shown in Ref. [22] that the inclusion of the OPE interactions had a strong impact on the location of the spin partner states of the $X(3872)$. In particular, the iterations of the OPE interaction to all orders were found to generate strong coupled-channel effects due to the then allowed transitions $D^*\bar{D}^* \leftrightarrow D^{(*)}\bar{D}$. As a consequence, the binding energy and the width of the spin-2 partner of the $X(3872)$ both appeared to be of the order of several dozens of MeV. Both values were found to be significantly larger than those reported in the literature earlier [31].

In this paper, a calculation for the spin partners of the Z_b states is presented in which the pole positions of the Z_b 's are treated as input. The underlying coupled-channel model includes short-range contact interactions, OPE, and OEE fully iterated to all orders. As our starting point, we assume both Z_b 's to be shallow bound states and investigate the role played by the spin symmetry violation introduced into the system via a nonzero value of the parameter δ defined in Eq. (1.13). In addition, we study the behaviour of the spin partners as the binding energies of the Z_b states are reduced (up to zero values) which allows us to make statements about the masses of the spin partners when the Z_b 's turn to virtual states. In particular, we find that the tensor spin partner W_{b2} with the quantum numbers 2^{++} survives in this limit *as a bound state* and it is expected to produce a visible resonant structure in the $B\bar{B}$ and $B\bar{B}^*$ line shapes a few MeV below the $B^*\bar{B}^*$ threshold.

The key aim of this study is to highlight explicitly the nontrivial impact of the non-perturbative one-pion exchange on the location of the spin partners of the Z_b states. For that it appears sufficient to base the study solely on the open-flavour channels introduced below. In particular, we neither include the inelastic channels ($\pi\Upsilon(nS)$ and $\pi h_b(mP)$) nor do we aim at a high accuracy description of the data. Clearly, as soon as the analysis of Refs. [17, 18] is refined to include one-pion exchange interactions, the predictions for the partner states could be refined further. Such a study, however, is beyond the scope of this paper.

The paper is organised as follows. In Sec. 2, we outline various implications of the heavy-quark spin symmetry (HQSS) in the purely contact theory. Then, in Sec. 3, we discuss the inclusion of the OPE interaction on top of the contact potential introduced in Sec. 2. The results obtained in the theory which incorporates both the contact and the OPE interactions are collected and discussed in Sec. 4. A peculiar alternative solution

found in the contact theory which, however, disappears from the theory once the OPE interaction is taken into account is highlighted in Sec. 5. We give an overview of the results obtained in the concluding Sec. 6.

2 Contact theory

We start from the purely contact theory. The basis of states — see Ref. [32] — can be adapted directly from the c -sector to the b -sector,

$$\begin{aligned}
0^{++} &: \{B\bar{B}(^1S_0), B^*\bar{B}^*(^1S_0)\}, \\
1^{+-} &: \{B\bar{B}^*(^3S_1, -), B^*\bar{B}^*(^3S_1)\}, \\
1^{++} &: \{B\bar{B}^*(^3S_1, +)\}, \\
2^{++} &: \{B^*\bar{B}^*(^5S_2)\}.
\end{aligned} \tag{2.1}$$

Here, the individual partial waves are labelled as $^{2S+1}L_J$ with S , L , and J denoting the total spin, the angular momentum, and the total momentum of the two-meson system, respectively. The C-parity eigenstates are defined as⁴

$$B\bar{B}^*(\pm) = \frac{1}{\sqrt{2}} (B\bar{B}^* \pm B^*\bar{B}) \tag{2.2}$$

and comply with the convention for the C-parity transformation $\hat{C}\mathcal{M} = \bar{\mathcal{M}}$.

In the basis of Eq. (2.1) and for a given set of the J^{PC} quantum numbers the leading-order EFT potentials $V_{\text{LO}}^{(JPC)}$ which respect the heavy-quark spin symmetry read [32–34]

$$V_{\text{LO}}^{(0^{++})} = \begin{pmatrix} C_{1a} & -\sqrt{3}C_{1b} \\ -\sqrt{3}C_{1b} & C_{1a} - 2C_{1b} \end{pmatrix} \equiv \frac{1}{4} \begin{pmatrix} 3C_1 + C'_1 & -\sqrt{3}(C_1 - C'_1) \\ -\sqrt{3}(C_1 - C'_1) & C_1 + 3C'_1 \end{pmatrix}, \tag{2.3}$$

$$V_{\text{LO}}^{(1^{+-})} = \begin{pmatrix} C_{1a} - C_{1b} & 2C_{1b} \\ 2C_{1b} & C_{1a} - C_{1b} \end{pmatrix} \equiv \frac{1}{2} \begin{pmatrix} C_1 + C'_1 & C_1 - C'_1 \\ C_1 - C'_1 & C_1 + C'_1 \end{pmatrix}, \tag{2.4}$$

$$V_{\text{LO}}^{(1^{++})} = C_{1a} + C_{1b} \equiv C_1, \tag{2.5}$$

$$V_{\text{LO}}^{(2^{++})} = C_{1a} + C_{1b} \equiv C_1, \tag{2.6}$$

where $\{C_{1a}, C_{1b}\}$ and $\{C_1, C'_1\}$ are two alternative sets of low-energy constants (contact terms).

With the help of the appropriate unitary transformations, the potential matrices (2.3) and (2.4) can be diagonalised to take the form $\text{diag}(C_1, C'_1)$. Therefore, in the strict heavy-quark limit ($\delta = 0$) and in the purely contact theory, if the potential $C_1^{(\prime)}$ is strong enough to bind the system in one channel, it is inevitably strong enough to produce bound state(s) in the sibling channel(s). Furthermore, since the binding energies in different channels are governed by the same combinations of the contact terms, the corresponding molecular states appear to be degenerate in mass. This observation allowed the authors of Refs. [22, 35] to

⁴In what follows, $B\bar{B}^*$ is used as a shorthand notation for the combination with the appropriate C-parity; the latter may be stated explicitly if necessary, like in Eq. (2.1).

predict, in the strict HQSS limit, the existence of multiple degenerate isosinglet states in the c -sector. Obviously, this conclusion trivially translates into the b -sector and holds for the isovector states, too. In particular, one finds

$$E_B^{(0)}[W_{b0}] = E_B^{(0)}[W_{b1}] = E_B^{(0)}[W_{b2}] = E_B^{(0)}[Z_b] \quad \text{and} \quad E_B^{(0)}[W'_{b0}] = E_B^{(0)}[Z'_b], \quad (2.7)$$

where the superscript (0) indicates the exact HQSS limit which implies the relation

$$\delta \ll E_B \ll m \quad (2.8)$$

between the spin symmetry violating parameter δ , the typical binding energy E_B in the Z_b and $W_{b,J}$ states, and the heavy-meson mass. Therefore, the input provided by the masses of the two Z_b states is sufficient to fix the parameters of the contact interaction at leading order. In Refs. [7, 19, 20, 36] a different relation between the relevant scales of the problem was assumed,

$$E_B \ll \delta \ll m, \quad (2.9)$$

while the contact interaction at this order was still treated as spin symmetric — see Eqs. (2.3)-(2.6). Then, the degeneracy (2.7) is lifted and instead one arrives at some relations between the binding momenta of the partners,

$$\gamma_{Z_b} = \gamma_{Z'_b}, \quad \gamma_{W_{b1}} = \gamma_{W_{b2}}, \quad \gamma_{W_{b0}} = \frac{\gamma_{Z_b} + \gamma_{W_{b1}}}{2}, \quad \gamma_{W'_{b0}} = \frac{3\gamma_{Z_b} - \gamma_{W_{b1}}}{2}, \quad (2.10)$$

which, in particular, yield the relations (1.11)-(1.12) for the widths. It should be noted that, to this order, the states Z'_b and W'_{b0} cannot yet decay into the (open) channels $B\bar{B}^*$ and $B\bar{B}$, respectively, and the widths (1.11)-(1.12) originate entirely from inelastic transitions. As was shown in Ref. [22], already at order $O(\delta)$, relations (2.10) acquire corrections linear with the cutoff introduced to regularise the divergent integrals in the Lippmann-Schwinger equations. Then, to absorb this cutoff dependence, the renormalisation in principle calls for the presence of HQSS violating contact interactions, in addition to the HQSS preserving potentials (2.3)-(2.6). Since the HQSS violating counter terms are not known, as an alternative approach, one may vary the cutoff in some reasonable range to estimate the uncertainty in the position of the partner states due to the omission of these interactions. In practice, the cutoff dependence appears to be very marginal (at least in the pionless theory) which can be, in part, justified by the large b -quark mass (much larger than the characteristic cutoff varied in the range from the pion mass and up to the chiral symmetry breaking scale ~ 1 GeV) and by the additional suppression of such terms by a factor γ/m (at least for the uncoupled partial waves) [22].

Note that the transitions $B^*\bar{B}^* \rightarrow B\bar{B}^*$ and $B^*\bar{B}^* \rightarrow B\bar{B}$ do not vanish already in the pionless theory, such that the coupled-channel dynamics for the states Z'_b and W'_{b0} produce an additional shift of the binding momenta and of the imaginary part of the order $O(\gamma^2/\sqrt{m\delta})$ [22]. Moreover, as it will be shown in this paper, once the OPE interaction is included, the state W_{b2} can also participate in the coupled-channel transitions, the latter having a significant impact on the location of this state.

3 One-pion exchange interaction

We start from the lowest-order nonrelativistic interaction Lagrangian [37, 38],

$$\mathcal{L} = \frac{g_b}{2f_\pi} \left(\mathbf{B}^{*\dagger} \cdot \nabla \pi^a \tau^a B + B^\dagger \tau^a \nabla \pi^a \cdot \mathbf{B}^* + i[\mathbf{B}^{*\dagger} \times \mathbf{B}^*] \cdot \nabla \pi^a \tau^a \right), \quad (3.1)$$

and employ the heavy-quark flavour symmetry to equate the dimensionless coupling constant g_b to the similar constant g_c which parametrises the $D^* D \pi$ vertex. It can be determined directly from the observable $D^* \rightarrow D \pi$ decay width via

$$\Gamma(D^{*+} \rightarrow D^+ \pi^0) = \frac{g_c^2 m_{D^+} q^3}{24\pi f_\pi^2 m_{D^{*+}}}, \quad (3.2)$$

where q is the centre-of-mass momentum in the final state. The numerical value extracted from data [9] reads

$$g_b = g_c \approx 0.57 \quad (3.3)$$

and it agrees within 10% with the recent lattice QCD determination of the $B^* B \pi$ coupling constant [39].

Depending on the channel, the OPE potential contains the pion propagator and two vertices of the type $B^* \rightarrow B^{(*)} \pi$ following directly from Lagrangian (3.1),

$$\begin{aligned} v^a(B^* \rightarrow B \pi) &= \frac{g_b}{2f_\pi} \tau^a (\boldsymbol{\epsilon} \cdot \mathbf{q}), \\ v^a(B^* \rightarrow B^* \pi) &= -\frac{g_b}{\sqrt{2}f_\pi} \tau^a (\mathbf{A} \cdot \mathbf{q}), \end{aligned} \quad (3.4)$$

where $\mathbf{A} = \frac{i}{\sqrt{2}}(\boldsymbol{\epsilon} \times \boldsymbol{\epsilon}'^*)$, $\boldsymbol{\epsilon}$ and $\boldsymbol{\epsilon}'^*$ stand for the polarisation vectors of the initial and final B^* mesons, \mathbf{q} is the pion momentum, τ^a is the isospin Pauli matrix, and $f_\pi = 92.2$ MeV is the pion decay constant — see also Refs. [22, 40]. Then, the OPE potentials connecting the heavy-meson $B^{(*)} B^{(*)}$ pairs in the initial and in the final state read⁵

$$\begin{aligned} V_{B\bar{B} \rightarrow B^* \bar{B}}(\mathbf{p}, \mathbf{p}') &= -\frac{2g_b^2}{(4\pi f_\pi)^2} \boldsymbol{\tau}_1 \cdot \boldsymbol{\tau}_2^c (\boldsymbol{\epsilon}_1 \cdot \mathbf{q})(\boldsymbol{\epsilon}_2'^* \cdot \mathbf{q}) \left(\frac{1}{D_{BB\pi}(\mathbf{p}, \mathbf{p}')} + \frac{1}{D_{B^* B^* \pi}(\mathbf{p}, \mathbf{p}')} \right), \\ V_{B\bar{B} \rightarrow B^* \bar{B}^*}(\mathbf{p}, \mathbf{p}') &= \frac{2\sqrt{2}g_b^2}{(4\pi f_\pi)^2} \boldsymbol{\tau}_1 \cdot \boldsymbol{\tau}_2^c (\mathbf{A}_1 \cdot \mathbf{q})(\boldsymbol{\epsilon}_2 \cdot \mathbf{q}) \left(\frac{1}{D_{BB^* \pi}(\mathbf{p}, \mathbf{p}')} + \frac{1}{D_{B^* B^* \pi}(\mathbf{p}, \mathbf{p}')} \right), \\ V_{B\bar{B} \rightarrow B^* \bar{B}^*}(\mathbf{p}, \mathbf{p}') &= -\frac{2g_b^2}{(4\pi f_\pi)^2} \boldsymbol{\tau}_1 \cdot \boldsymbol{\tau}_2^c (\boldsymbol{\epsilon}_1'^* \cdot \mathbf{q})(\boldsymbol{\epsilon}_2'^* \cdot \mathbf{q}) \left(\frac{2}{D_{BB^* \pi}(\mathbf{p}, \mathbf{p}')} \right), \\ V_{B^* \bar{B}^* \rightarrow B^* \bar{B}^*}(\mathbf{p}, \mathbf{p}') &= -\frac{4g_b^2}{(4\pi f_\pi)^2} \boldsymbol{\tau}_1 \cdot \boldsymbol{\tau}_2^c (\mathbf{A}_1 \cdot \mathbf{q})(\mathbf{A}_2 \cdot \mathbf{q}) \left(\frac{2}{D_{B^* B^* \pi}(\mathbf{p}, \mathbf{p}')} \right), \end{aligned} \quad (3.5)$$

where \mathbf{p} (\mathbf{p}') denotes the centre-of-mass momentum of the initial (final) heavy-meson pair and the pion momentum is $\mathbf{q} = \mathbf{p} + \mathbf{p}'$. For the isovector states, the isospin factor which appears from the operator $\boldsymbol{\tau}_1 \cdot \boldsymbol{\tau}_2^c$ is

$$\boldsymbol{\tau}_1 \cdot \boldsymbol{\tau}_2^c = [3 - 2I(I+1)]_{I=1} = -1, \quad (3.6)$$

⁵ Note that we use a convention where the integration weight is absorbed into the potential. Accordingly, the usual factor $(2\pi)^3$ does not appear in the integral equation (3.12) given below.

where $\boldsymbol{\tau}^c$ stands for the generator of the antifundamental representation, $\boldsymbol{\tau}^c = \tau_2 \boldsymbol{\tau}^T \tau_2 = -\boldsymbol{\tau}$. Note that in contrast to what is given above, in the isoscalar channel, studied, for example, in Ref. [22], the isospin factor is +3.

Furthermore, the expressions for the propagators in Eq. (3.5) read

$$D_{BB^*\pi}(\mathbf{p}, \mathbf{p}') = 2E_\pi(\mathbf{q}) \left(m + m_* + \frac{\mathbf{p}^2}{2m} + \frac{\mathbf{p}'^2}{2m_*} + E_\pi(\mathbf{q}) - \sqrt{s} \right), \quad (3.7)$$

$$D_{BB\pi}(\mathbf{p}, \mathbf{p}') = 2E_\pi(\mathbf{q}) \left(m + m + \frac{\mathbf{p}^2}{2m} + \frac{\mathbf{p}'^2}{2m} + E_\pi(\mathbf{q}) - \sqrt{s} \right), \quad (3.8)$$

$$D_{B^*B^*\pi}(\mathbf{p}, \mathbf{p}') = 2E_\pi(\mathbf{q}) \left(m_* + m_* + \frac{\mathbf{p}^2}{2m_*} + \frac{\mathbf{p}'^2}{2m_*} + E_\pi(\mathbf{q}) - \sqrt{s} \right), \quad (3.9)$$

where $E_\pi = \sqrt{\mathbf{q}^2 + m_\pi^2}$ is the pion energy and \sqrt{s} defines the total energy of the system which is conveniently represented as $\sqrt{s} = m + m_* + E$, with E counted with respect to the $B\bar{B}^*$ threshold. The time-reversed transition potentials are trivially obtained from Eqs. (3.5) by interchanging \mathbf{p} and \mathbf{p}' and using that $D_{B^*B\pi}(\mathbf{p}, \mathbf{p}') = D_{BB^*\pi}(\mathbf{p}', \mathbf{p})$.

The three-body effects are incorporated in the above OPE potentials via the heavy-meson recoil corrections and via the energy-dependent terms in the time-ordered propagators from Eqs. (3.7)-(3.9). The leading-order static OPE potentials are then easily obtained from the full results by neglecting the three-body terms, that is by the replacement

$$\frac{1}{D_{B^{(*)}B^{(*)}\pi}(\mathbf{p}, \mathbf{p}')} + \frac{1}{D_{B^{(*)}B^{(*)}\pi}(\mathbf{p}, \mathbf{p}')} \rightarrow 2 \times \frac{1}{2E_\pi^2(\mathbf{q})} = \frac{1}{\mathbf{q}^2 + m_\pi^2}. \quad (3.10)$$

We checked numerically that, for the mass spectra which are the focus of this work, the three-body terms are basically irrelevant. Accordingly, one could as well have used the static pion propagators. The reason is that the B^*-B mass difference δ — see Eq. (1.13) — is about three times smaller than the pion mass and, therefore, there are no three-body cuts located in the vicinity of $B^{(*)}B^{(*)}$ thresholds. This situation is, however, very different in the c -sector: the $D\bar{D}\pi$ threshold lies about 7 MeV below the $D\bar{D}^*$ threshold and, hence, three-body effects play a prominent role for understanding the dynamics of the $X(3872)$ state treated as a $D\bar{D}^*$ molecule [27, 28, 30].

The OEE can be calculated straightforwardly from the expressions given above if one makes the following replacements: (i) the isospin factor of Eq. (3.6) by +1; (ii) the pion mass by the η mass, and (iii) the pion coupling constant g_c by the η coupling constant $g_c/\sqrt{3}$ which can be found, for example, in Ref. [41].

As soon as the OPE potential is included, it enables transitions to D and even G waves which, therefore, have to be included in the extended set of basis states,

$$\begin{aligned} 0^{++} &: \{B\bar{B}(^1S_0), B^*\bar{B}^*(^1S_0), B^*\bar{B}^*(^5D_0)\}, \\ 1^{+-} &: \{B\bar{B}^*(^3S_1, -), B\bar{B}^*(^3D_1, -), B^*\bar{B}^*(^3S_1), B^*\bar{B}^*(^3D_1)\}, \\ 1^{++} &: \{B\bar{B}^*(^3S_1, +), B\bar{B}^*(^3D_1, +), B^*\bar{B}^*(^5D_1)\}, \\ 2^{++} &: \{B\bar{B}(^1D_2), B\bar{B}^*(^3D_2), B^*\bar{B}^*(^5S_2), B^*\bar{B}^*(^1D_2), B^*\bar{B}^*(^5D_2), B^*\bar{B}^*(^5G_2)\}. \end{aligned} \quad (3.11)$$

As before, the C-parity of the states is indicated explicitly in parentheses whenever necessary.

The coupled-channel integral equations for the scattering amplitude take the form

$$a_{ij}^{(JPC)}(p, p') = V_{ij}^{(JPC)}(p, p') - \sum_n \int dk k^2 V_{in}^{(JPC)}(p, k) G_n(k) a_{nj}^{(JPC)}(k, p'), \quad (3.12)$$

where i, j , and n label the basis vectors, as they appear in Eq. (3.11), and

$$G_n = (k^2 / (2\mu_n) + m_{1,n} + m_{2,n} - \sqrt{s} - i\epsilon)^{-1}, \quad \mu_n = \frac{m_{1,n} m_{2,n}}{m_{1,n} + m_{2,n}} \quad (3.13)$$

are the propagator and the reduced mass of the heavy meson-antimeson pair in the given channel evaluated in its centre of mass. The potential $V_{ij}^{(JPC)}(p, p')$ includes the contact term as well as the meson exchange interactions in the channel with the given quantum numbers J^{PC} and in the given partial wave. The Lippmann-Schwinger-type equations derived are regularised with the sharp cutoff, where the value of the latter is chosen to be of the order of a natural hard scale in the problem — see Ref. [22]. All necessary details of the coupled-channel formalism, of the partial wave projection, and so on can be found in Refs. [22, 42]. However, it is important to pinpoint a crucial difference between the potentials used in Refs. [22] and the ones from this work: while the OPE potential from Ref. [22] describes the interaction in the isosinglet channels, here it operates in the isovector systems. Thus, the trivial modification one needs to make in the equations is to change the isospin coefficient 3, which multiplies the OPE potential in the isosinglet channels, for the isospin coefficient -1, which corresponds to the isovector channels — see Eq. (3.6). In addition, it has to be noticed that the sign of the OPE potential also depends on the C-parity of the system. Then, as a net result, the central (S -wave) part of the OPE potential is attractive in the C-odd Z_b 's channel while it is repulsive in the C-even channels where the W_{bJ} states are predicted. It is important to note, however, that the net effect of the OPE can be attractive also in those channels due to the nondiagonal transition potentials — in particular, due to the S - D transitions induced by the tensor force.

The inclusion of the OPE interaction modifies the potentials (2.3)-(2.6). Nevertheless, as demonstrated in Ref. [22], in the strict heavy-quark limit, if all coupled channels and all relevant partial waves are taken into account, for a given set of quantum numbers J^{PC} , one can find the unitary operator that block diagonalises the potential into the form (for the sake of transparency, the size of the blocks is quoted explicitly in parentheses),

$$\begin{aligned} \tilde{V}^{(0^{++})}(3 \times 3) &= A(2 \times 2) \oplus B(1 \times 1), \\ \tilde{V}^{(1^{+-})}(4 \times 4) &= A(2 \times 2) \oplus B(1 \times 1) \oplus C(1 \times 1), \\ \tilde{V}^{(1^{++})}(3 \times 3) &= A(2 \times 2) \oplus D(1 \times 1), \\ \tilde{V}^{(2^{++})}(6 \times 6) &= A(2 \times 2) \oplus D(1 \times 1) \oplus E(3 \times 3). \end{aligned} \quad (3.14)$$

This conclusion does not depend on the isospin of the system and it is, therefore, equally valid for both isosinglets and isovectors. Since the contact interactions contribute to both matrix A (via $C_1 = C_{1a} + C_{1b}$) and matrix B (via $C'_1 = C_{1a} - 3C_{1b}$) and since at least one of these two matrices enters all four potentials for all quantum numbers one expects that the existence of the Z_b and Z'_b as bound states in the 1^{+-} channel entails the existence of

the bound states in the other three channels, too, with the degeneracy pattern given by Eq. (2.7) as in case of the purely contact theory. As explained in the previous section, this pattern is expected to be lifted as soon as the physical masses of the B and B^* mesons are used in the calculations. Meanwhile, the HQSS constraints are still expected to work quite well for the contact potentials.

4 Results and discussion

In this section, we present and discuss the results of our calculations with special emphasis on the role of the pion dynamics for the location of the poles of the W_{bJ} 's — the spin partners of the Z_b states. Furthermore, motivated by the fact that in the isovector channel the relative importance of the η -exchange is larger than in the isoscalar channel, we also include it explicitly in our calculations.

As our starting point, we assume both Z_b and Z'_b to be shallow bound states and treat their binding energies as input parameters. This allows us to fix completely the HQSS-constrained leading-order contact potential — see Eqs. (2.3)-(2.6). For definiteness, as an example, we fix the binding energies of the Z_b 's to be

$$E_B(B^*\bar{B})[Z_b] = 5 \text{ MeV}, \quad E_B(B^*\bar{B}^*)[Z'_b] = 1 \text{ MeV}, \quad (4.1)$$

in line with Ref. [16]. For both Z_b 's the energy is counted relative to the respective reference threshold explicitly stated in Eq. (4.1) in parentheses. Ideally, one would need to extract pole locations and residues for the spin partner states of the Z_b 's directly from the calculated T -matrices. However, this requires an analytic continuation of the amplitudes into the complex plane that goes beyond the scope of the present paper. Therefore, to extract the binding energies and the widths of the spin partners, W_{bJ} 's, we mimic the experimental procedure and calculate the production rates in the elastic channels for the spin partner states. In what follows, similarly to Eq. (4.1), the binding energies of the partner states will be always defined relative to their reference thresholds, namely,

Threshold:	Spin partner:	
$B\bar{B}$	$W_{b0}(0^{++})$,	(4.2)
$B\bar{B}^*$	$W_{b1}(1^{++})$,	
$B^*\bar{B}^*$	$W'_{b0}(0^{++})$, $W_{b2}(2^{++})$.	

4.1 Dependence on the HQSS breaking scale

To highlight the impact of the OPE and OEE on the pole locations of the spin partner states, in Fig. 1, we show the evolution of the extracted binding energies as functions of δ — the HQSS breaking mass splitting between the B and B^* mesons — for four different scenarios:

- Scenario A: purely contact potential;
- Scenario B: contact potential plus the central (S -wave) OPE interaction;

- Scenario C: contact potential plus the full OPE interaction;
- Scenario D: contact potential plus the full OPE and OEE interactions altogether.

It follows from Eqs. (2.7) and (3.14) that, in the strict HQSS limit ($\delta = 0$), the Z_b 's and the W_{bJ} 's populate two families of states and that this conclusion holds both with and without OPE and OEE interactions included. Given the input from Eq. (4.1), this explains why, for all four scenarios above, the 2^{++} , 1^{++} , and one of the 0^{++} states have the same binding energy $E_B = 5$ MeV while the other 0^{++} spin partner has the binding energy $E_B = 1$ MeV in this limit. However, for $\delta > 0$, HQSS is lifted and the exact degeneracy (2.7) is lost — see the discussion in Secs. 2 and 3 above. Then, as δ grows from zero to the physical value of 45 MeV, the spin partners from the first family (W_{b0} , W_{b1} , and W_{b2}) tend to become more bound while the state W'_{b0} becomes unbound fast and its pole moves to the second Riemann sheet.⁶ Note that while varying δ we keep adjusting the parameters of the contact potential such that the pole locations of Z_b and Z'_b stay fixed at the values given in Eqs. (4.1).

From Fig. 1 one can conclude that the central (S -wave) part of the OPE has no influence on the position of the poles⁷ while its tensor part has a significant impact, especially on the 2^{++} state W_{b2} . Indeed, due to the additional attraction which stems from the OPE-related tensor forces, the binding energy of the W_{b2} grows by almost a factor of two as compared to the results of the pionless theory (from 13 to 23 MeV). Furthermore, by comparing the results in the strict HQSS limit ($\delta = 0$) with those for the physical mass splitting ($\delta = 45$ MeV), one can conclude that spin symmetry is violated quite strongly and that a substantial amount of this violation for the 2^{++} state stems from the tensor forces.

Finally, it can also be seen in Fig. 1 that the η -exchange does not play a prominent role for the systems under study, for it only slightly diminishes the OPE. This can be seen in all four plots in Fig. 1.

4.2 Dependence on the one-boson-exchange strength parameter

To further illustrate the role played by the dynamics governed by the pion and η -meson exchanges, in Fig. 2, we plot the variation of the binding energies for the spin partners W_{bJ} with the coupling constant g_b varied from 0 (the results of the purely contact theory are naturally recovered in this limit) to its physical value quoted in Eq. (3.3). In this calculation, the masses of the B and B^* mesons are fixed to their physical values [9]. One can draw several conclusions from Fig. 2. On the one hand, for all values of g_b the effect of the central S -wave OPE potential can always be absorbed completely into the contact terms. Indeed, in all plots, the blue dashed line behaves like a constant. On the other

⁶Strictly speaking, the 0^{++} state residing near the $B^*\bar{B}^*$ threshold should be regarded as a resonance since it appears above the $B\bar{B}$ and $B\bar{B}^*$ thresholds and the corresponding pole acquires an imaginary part. Nevertheless, for clarity, we still refer to it as to a bound or virtual state with respect to the $B^*\bar{B}^*$ threshold and use the language of the corresponding two-sheet Riemann surface.

⁷More rigorously, the S -wave part of the OPE is absorbed into the contact interactions via the re-fit of the latter to preserve the location of the Z_b poles.

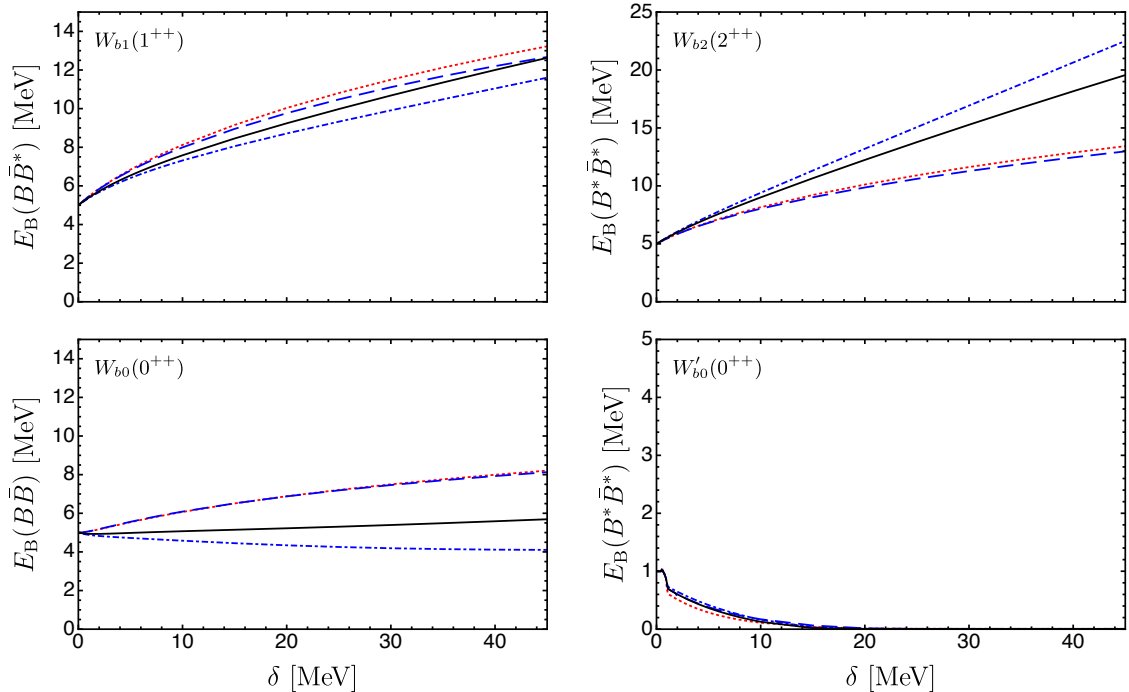


Figure 1. Evolution of the binding energies of the Z_b 's spin partners calculated with and without π - and η -meson exchanges as functions of the mass splitting δ between the B^* and B mesons. The contact terms are re-fitted for each value of δ to provide the given binding energies of the Z_b and Z'_b states used as input — see Eq. (4.1). The binding energies of the W_{bJ} states are defined relative to their reference thresholds quoted in parentheses. The red dotted curves correspond to the pionless (purely contact) theory — Scenario A; the blue dashed curves are obtained for the central (S -wave) part of the OPE included — Scenario B; the blue dashed-dotted lines represent the results for the full OPE, including tensor forces — Scenario C; the black solid curves show the results of the full calculation with both OPE and OEE included on top of the contact interactions — Scenario D. The physical limit corresponds to the right edge of the plots. The results are obtained with the sharp cutoff $\Lambda = 1$ GeV in the integral equations (3.12). The uncertainty caused by the residual Λ -dependence of the equations can be estimated using the results presented in Table 1.

hand, starting from $g_b \simeq 0.3$, the dashed-dotted line starts to deviate from the dashed line indicating that the role of the tensor forces increases fast thus providing a substantial shift in the binding energy in the physical limit for the g_b — this effect is best seen for the tensor partner W_{b2} .

4.3 Dependence on the input for the Z_b 's binding energies

Finally, we investigate the dependence of the binding energies of the spin partners W_{bJ} 's on the input used for binding energies of the Z_b 's. To simplify the presentation of the results, we choose coinciding binding energies of the latter and vary them in a sufficiently wide range compatible with the values found in the literature. The results for the binding energies of the spin partners W_{bJ} 's are given in Fig. 3. To guide the eye, the constraint $E_B[Z'_b] = E_B[Z_b]$ is shown by the grey dashed line. Furthermore, we consider the limit

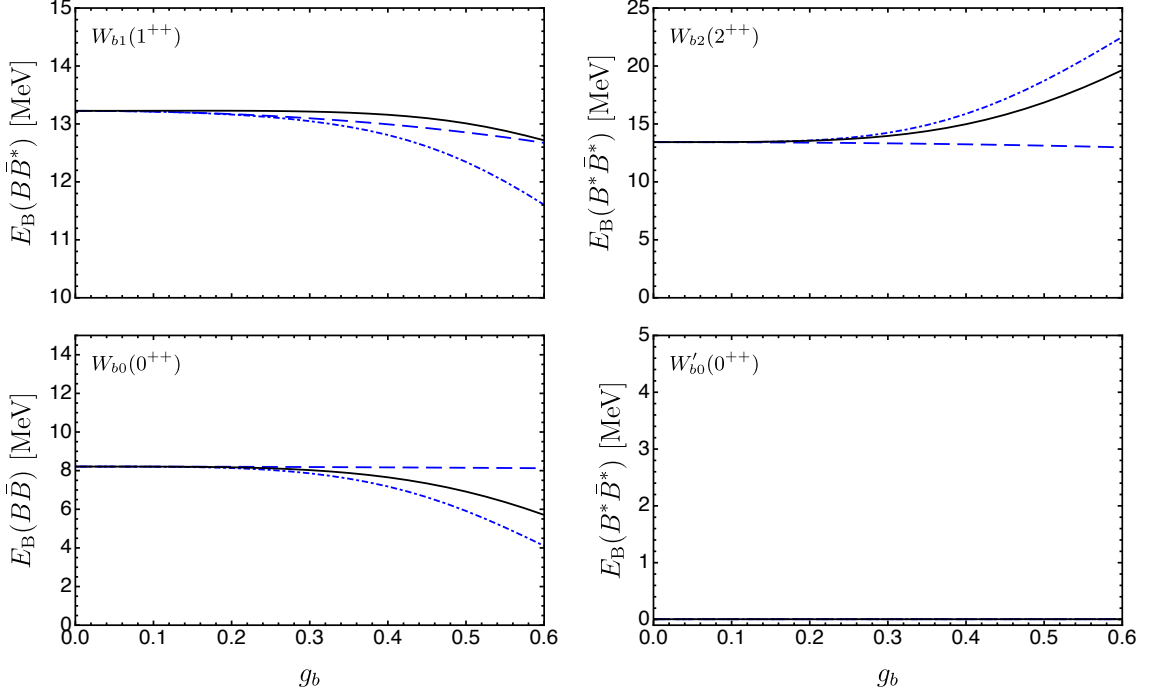


Figure 2. The binding energies of the Z_b 's spin partners as functions of the coupling constant g_b for the physical mass splitting δ between B^* and B mesons. The binding energies of the Z_b and Z'_b states are used as input — see Eq. (4.1). The notation of curves is the same as in Fig. 1. The results are obtained with the sharp cutoff $\Lambda = 1$ GeV in the integral equations (3.12).

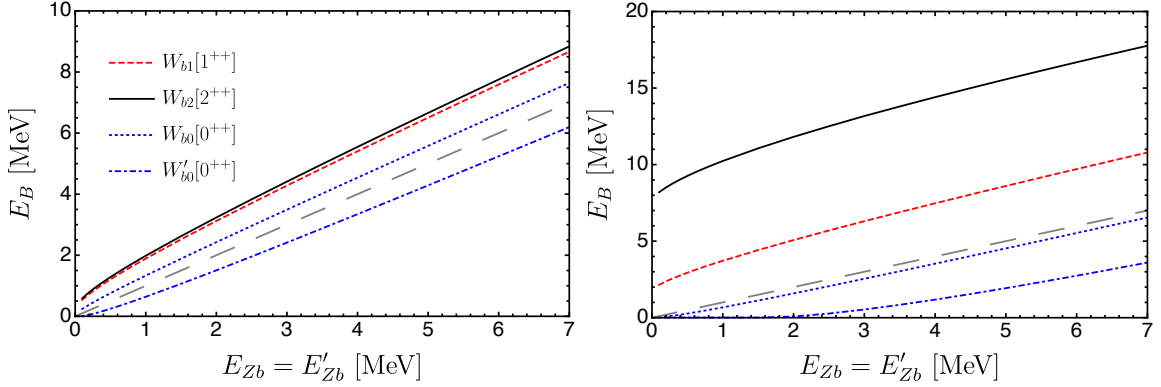


Figure 3. Dependence of the binding energies of the $W_{b,J}$'s on the input used for the binding energies of the Z_b 's for the purely contact interaction (the first plot) and for the full theory, including the OPE and OEE (the second plot). To guide the eye, the (equal) binding energies of the Z_b 's are shown as the grey dashed lines. The results are obtained with the sharp cutoff $\Lambda = 1$ GeV in the integral equations (3.12).

$E_B[Z'_b] = E_B[Z_b] \rightarrow 0$ which provides a smooth matching between the case of the Z_b 's as bound states and as virtual levels. The results for the widths of the partners are shown in Fig. 4. It is instructive to note that, in agreement with Eq. (2.7), in the strict HQSS

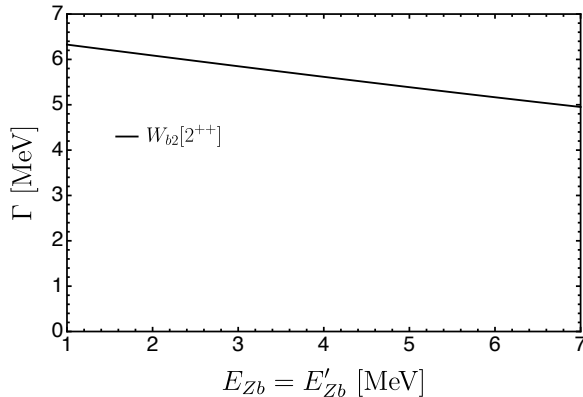


Figure 4. The decay width of the $W_{b2}(2^{++})$ state from coupled-channel transitions $B^*\bar{B}^* \rightarrow B\bar{B}$ and $B^*\bar{B}^* \rightarrow B\bar{B}^*$ evaluated in the full theory, including the OPE and OEE.

limit and for $E_B[Z_b] = E_B[Z'_b]$, all six partner states are strictly degenerate. Therefore, deviations of the curves for the spin partner states W_{bJ} 's from the grey dashed line in Fig. 3 illustrate the importance of the HQSS breaking corrections related to the nonvanishing B^* - B mass splitting. In particular, had the strict HQSS limit been realised in nature all six spin partner states would have become unbound in unison for $E_B[Z_b] = E_B[Z'_b] \rightarrow 0$. Actually, as it is seen from the left plot in Fig. 3, a similar pattern is observed in the purely contact theory beyond the strict HQSS limit. On the other hand, in the full theory with pions and η -mesons (see the right plot in Fig. 3), the 1^{++} and 2^{++} partners survive as bound states in the limit $E_B[Z_b] = E_B[Z'_b] \rightarrow 0$ when both Z_b 's turn to virtual levels. The width of the 2^{++} state is expected at the level of a few MeV — see Fig. 4 — so that one should be able to resolve it from the $B^*\bar{B}^*$ threshold. Meanwhile, the poles for both 0^{++} partners move to the unphysical Riemann sheets.

We note that the inclusion of the OPE interaction leads to selfconsistent results only if all relevant partial waves as well as particle channels which are coupled via the pion-exchange potential are taken into account. Conversely, the partial neglect of the coupled-channel dynamics not only significantly affects the predictions for the partner states but also leads to the regulator(cutoff)-dependent results already in the strict HQSS limit. This is in full agreement with the results in the c -quark sector reported in Ref. [22].

In agreement with the discussion in Sec. 2, the results of the full coupled-channel problem beyond the HQSS limit may also exhibit some cutoff dependence which is however quite mild and which can be absorbed into a redefinition of higher-order HQSS violating contact interactions. To illustrate that the effect of the cutoff variation on our results is minor, in Table 1 we estimate the uncertainty in the binding energies and widths of the partner states when the cutoff is varied in the range from 800 to 1500 MeV.

Note that, in the vicinity of the peak, the energy dependence of the line shape for the 2^{++} partner state has a clear Breit-Wigner form, from which the parameters quoted in Table 1 were extracted. On the contrary, since the Z'_b state resides very close to the $B^*\bar{B}^*$ threshold, the Breit-Wigner distribution in the resonance region is strongly distorted by threshold effects. Then, to arrive at the quantity that can be compared to the width from

	$Z_{b1}(1^{+-})$	$Z'_{b1}(1^{+-})$	$W_{b0}(0^{++})$	$W'_{b0}(0^{++})$	$W_{b1}(1^{++})$	$W_{b2}(2^{++})$
E_B [MeV]	5 (input)	1 (input)	5.3 ± 1.7	—	12.4 ± 0.6	19.8 ± 2.2
Γ_B [MeV]	—	—	—	—	—	4.6 ± 1.0
E_B [MeV]	1 (input)	1 (input)	0.7 ± 0.5	—	3.8 ± 0.1	10.2 ± 1.8
Γ_B [MeV]	—	—	—	—	—	6.2 ± 1.1

Table 1. The binding energies and the widths of the spin partners for the two sets of the Z_b and Z'_b binding energies used as input parameters. The uncertainty in the results is due to the variation of the cutoff in the Lippmann-Schwinger equations from 800 to 1500 MeV.

experiment one would need to convolute the energy distribution from the coupled-channel amplitudes with the resolution function, integrate it over the energy bins and then analyse with the standard Breit-Wigner techniques. Since this goes beyond the scope of the current work, we do not quote the width of the Z'_b in Table 1.

5 Comment on the pionless theory

In the previous section, we demonstrated that nonperturbative pion exchange has a significant impact on the pole locations of the spin partner states for the Z_b and Z'_b . In this section, we show that it plays an additional important role to identify correctly the realistic solution from the pair of solutions present in the purely contact theory as long as input from the 1^{+-} channel is used to fix the parameters. Indeed, in the potential (2.4) written in terms of the low-energy constants C_1 and C'_1 , an interchange of the latter only changes the sign of the off-diagonal elements which has no effect on the observables as long as Eq. (2.4) is the only contribution to the potential. Therefore, in the purely contact theory there are two solutions that both lead to the same masses of the Z_b states. Accordingly, there is an alternative solution to the one given in Eq. (2.7) for the spin partner states in the strict HQSS limit, namely

$$\text{Sol.2: } E_B^{(0)}[Z_b] = E_B^{(0)}[W_{b0}] \quad \text{and} \quad E_B^{(0)}[Z'_b] = E_B^{(0)}[W'_{b0}] = E_B^{(0)}[W_{b1}] = E_B^{(0)}[W_{b2}]. \quad (5.1)$$

The two solutions presented in Eqs. (2.7) and (5.1) and their evolution for finite δ 's are different in a nontrivial way. This is demonstrated in Fig. 5 where, for definiteness, we used Eq. (4.1) as input for the Z_b 's.⁸ However, as soon as the pion exchange is added, the strength of the off-diagonal elements changes and the system gets sensitive to the interchange $C_1 \leftrightarrow C'_1$. It turns out that, in the presence of the OPE with its physical strength (3.3), the Z_b 's binding energies can be fixed to their physical values only for the first solution which in the strict HQSS limit corresponds to Eq. (2.7) and which is discussed in the previous section. Thus, the OPE naturally removes an ambiguity from the predictions for the spin partner states.

⁸Cusp-like structures in the binding energies seen in Figs. 1 and 5 at small δ 's appear when, depending on the channel, the binding energy of the Z'_b used as input coincides with δ (that is with the mass difference between the $B\bar{B}$ and $B\bar{B}^*$ or $B\bar{B}^*$ and $B^*\bar{B}^*$ thresholds) or with 2δ (the splitting between the $B\bar{B}$ and $B^*\bar{B}^*$ thresholds).

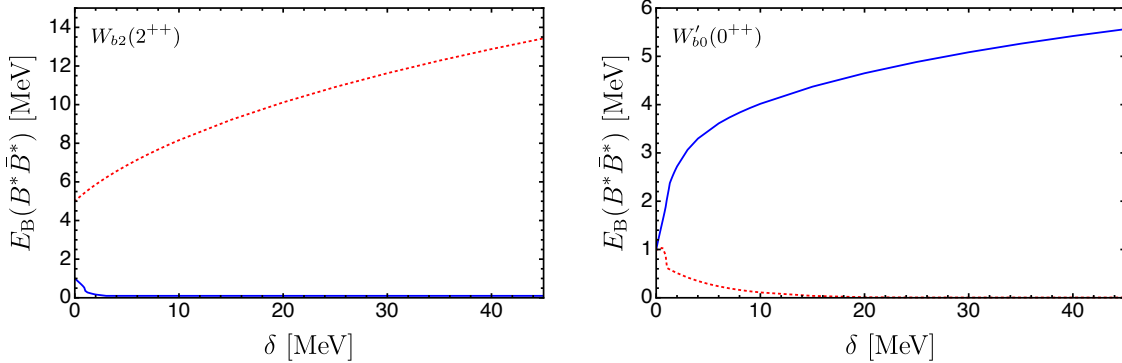


Figure 5. Binding energies of the $W_{b2}(2^{++})$ and $W'_{b0}(0^{++})$ states versus the mass splitting δ for two different solutions for the contact terms in the pionless theory: the red dotted lines correspond to the first solution discussed in Sec. 4 while the blue solid lines represent the results of the alternative scenario with the interchanged contact terms (see the text for the further details).

6 Conclusions

In this paper, we study the spin partners of the isovector bottomonium-like states $Z_b(10610)$ and $Z_b(10650)$ in the molecular model. For definiteness, we assume both Z_b states to be shallow bound states and treat their binding energies as input parameters of the model. This allows us to fix two low-energy constants describing the leading-order short-range interactions in the 1^{+-} channel. Then HQSS is used to construct the contact potentials for the spin partner states of the Z_b and Z'_b with the quantum numbers J^{++} ($J = 0, 1, 2$), conventionally denoted as W_{bJ} ($J = 0, 1, 2$). Motivated by the important role played by the nonperturbative pion dynamics in nuclear chiral EFTs — especially in the deuteron channel which demonstrates certain similarities to the Z_b states (see, for example, Refs. [25, 26]) — and in the c -quark sector [22], we performed a fully nonperturbative calculation with the one-pion exchange interaction added to the short-range terms. In addition, we include one- η exchange, also iterated to all orders for the sake of completeness, to see if it indeed diminishes the effect of the OPE as claimed in the literature [24].

Our results revealing the influence of the OPE and OEE interactions on the properties of the bottomonium-like systems under study can be summarised as follows.

- In contrast to the charmonium-like systems — see, for example, Refs. [22, 30] — three-body effects in the bottomonium sector play basically no role and, in analogy with the NN problem, they can be treated perturbatively. The reason why the static approximation for the OPE works well in the bottomonium-like systems is twofold: first, the B^*-B mass splitting is significantly smaller than the pion mass; second, the masses of the B mesons are large enough to make the typical three-body momenta (proportional to $\sqrt{m_\pi/m} \times \text{soft scale}$ — see, for example, Refs. [43, 44] for the details) sufficiently small compared to the other relevant scales of the problem such as the binding momenta and the pion mass.
- D waves (particularly the S - D transitions) play an important role and cannot be

disregarded. On the contrary, if only the central S -wave part of the OPE interaction is retained, the problem is practically indistinguishable from the purely contact one *after the parameters of the system are re-adjusted* to place the Z_b poles, used as input, to the prescribed locations. Since the leading non-trivial effect from the pions stems from the S - D tensor forces, the perturbative inclusion of the OPE is not sufficient.

- In agreement with the results of Ref. [22], the inclusion of the OPE interaction leads to selfconsistent results only if all relevant partial waves as well as particle channels which are coupled via the pion-exchange potential are taken into account. Due to the larger b -quark mass compared to the c -quark mass, consequences of uncontrolled omissions of partial waves are not that severe in the bottomonium sector. However, any partial neglect of this kind results in a strong cutoff dependence which reduces noticeably the predictive power of the approach.
- The most important effect of the coupled-channel dynamics reveals itself in the 2^{++} channel where, due to the $B^*\bar{B}^* \leftrightarrow B^{(*)}\bar{B}$ transitions driven by the S - D tensor forces from the OPE, the corresponding partner state W_{b2} acquires a width at the level of a few MeV and it remains bound even in the limit of vanishing binding energies of the Z_b states.
- One- η exchange, iterated to all orders, plays a minor role for the problem at hand slightly diminishing the effect of the OPE.

We, therefore, confirm the results of our previous studies of the OPE interaction which demonstrate its sizeable effect on the properties of the near-threshold resonances — see, for example, Refs. [22, 30]. On the other hand, our findings suggest that the claim made in Ref. [45] that the influence of the static S -wave OPE on the line shapes of the Z_b states can be as large as 30% is not correct. On the contrary, one expects that also for the line shapes the effect of the central S -wave OPE interaction can be largely absorbed into re-definition of the parameters of the model. However, we delegate a detailed investigation of the line shapes, which calls for an inclusion of the inelastic channels, to a later work.

The predicted masses of the spin partners of the Z_b states are quoted in Table 1. In the same table we give the width of the W_{b2} state due to the coupled-channel transitions to the open-flavour channels $B\bar{B}$ and $B\bar{B}^*$. From this table one can conclude that three sibling states with the quantum numbers 0^{++} , 1^{++} , and 2^{++} are expected to exist near the $B\bar{B}$, $B\bar{B}^*$, and $B^*\bar{B}^*$ thresholds, respectively, and to produce visible peak-like structures in the line shapes. A similar 0^{++} state near the $B^*\bar{B}^*$ threshold has the pole located on a remote Riemann sheet. It remains to be seen whether or not this state can be observed experimentally.

The probably most important finding of this work is that we predict the existence of an isovector 2^{++} tensor state lying a few MeV below the $B^*\bar{B}^*$ threshold. Unlike its scalar partner states, this tensor state should reveal itself as *a bound-state* peak in the $B^*\bar{B}^*$ line shape even in the limit of vanishing binding energies of the Z_b states. The width of this structure is expected at the level of a few MeV so in principle one should be able to resolve it in the experiment.

It should be stressed, however, that in this work we did not include any inelastic channels. The W_{b2} width just reported — see Table 1 — stems from the possible decays of the W_{b2} to the $B\bar{B}^{(*)}$ final states in D waves. Therefore, the total width of this state should be somewhat bigger due to its decays to, for example, $\Upsilon(nS)\rho$, as proposed in Ref. [21], or to $\chi_{b1}\pi$ and $\chi_{b2}\pi$. However, since inelastic channels play only a minor role for the Z_b 's, it is also natural to expect their contribution to be small enough for the W_{b2} which must make this state resolvable from the threshold and, therefore, detectable in the line shape.

Acknowledgments

The authors are grateful to R. V. Mizuk for enlightening discussions and to F.-K. Guo for reading the manuscript and for valuable comments. This work is supported in part by the DFG and the NSFC through funds provided to the Sino-German CRC 110 “Symmetries and the Emergence of Structure in QCD” (NSFC Grant No. 11261130311). Work of A. N. was performed within the Institute of Nuclear Physics and Engineering supported by MEPhI Academic Excellence Project (contract No 02.a03.21.0005, 27.08.2013). He also acknowledges support from the Russian Foundation for Basic Research (Grant No. 17-02-00485). Work of V. B. is supported by the DFG (Grant No. GZ: BA 5443/1-1).

References

- [1] BELLE collaboration, S. K. Choi et al., *Observation of a narrow charmonium-like state in exclusive $B^\pm \rightarrow K^\pm \pi^+ \pi^- J/\psi$ decays*, *Phys. Rev. Lett.* **91** (2003) 262001, [[hep-ex/0309032](#)].
- [2] N. Brambilla et al., *Heavy quarkonium: progress, puzzles, and opportunities*, *Eur. Phys. J.* **C71** (2011) 1534, [[1010.5827](#)].
- [3] S. Eidelman, *Recent Progress in Charmonium Studies*, *Acta Phys. Polon.* **B47** (2016) 109–116.
- [4] BELLE collaboration, A. Bondar et al., *Observation of two charged bottomonium-like resonances in $\Upsilon(5S)$ decays*, *Phys. Rev. Lett.* **108** (2012) 122001, [[1110.2251](#)].
- [5] BELLE collaboration, I. Adachi et al., *Study of Three-Body $Y(10860)$ Decays*, 2012. [1209.6450](#).
- [6] BELLE collaboration, A. Garmash et al., *Observation of $Z_b(10610)$ and $Z_b(10650)$ Decaying to B Mesons*, *Phys. Rev. Lett.* **116** (2016) 212001, [[1512.07419](#)].
- [7] A. E. Bondar, A. Garmash, A. I. Milstein, R. Mizuk and M. B. Voloshin, *Heavy quark spin structure in Z_b resonances*, *Phys. Rev.* **D84** (2011) 054010, [[1105.4473](#)].
- [8] F. K. Guo, C. Hanhart, U.-G. Meißner, Q. Wang, Q. Zhao and B. S. Zou, arXiv:1705.00141 [[hep-ph](#)].
- [9] PARTICLE DATA GROUP collaboration, C. Patrignani et al., *Review of Particle Physics*, *Chin. Phys.* **C40** (2016) 100001.
- [10] BELLE collaboration, I. Adachi, *Observation of two charged bottomonium-like resonances, in Flavor physics and CP violation. Proceedings, 9th International Conference, FPCP 2011, Maale HaChamisha, Israel, May 23-27, 2011*, 2011. [1105.4583](#).

- [11] BELLE collaboration, A. Garmash et al., *Amplitude analysis of $e^+e^- \rightarrow \Upsilon(nS)\pi^+\pi^-$ at $\sqrt{s} = 10.865$ GeV*, *Phys. Rev.* **D91** (2015) 072003, [[1403.0992](#)].
- [12] C. Hanhart, J. R. Pelaez and G. Rios, *Remarks on pole trajectories for resonances*, *Phys. Lett.* **B739** (2014) 375–382, [[1407.7452](#)].
- [13] A. Esposito, A. Pilloni and A. D. Polosa, *Hybridized Tetraquarks*, *Phys. Lett.* **B758** (2016) 292–295, [[1603.07667](#)].
- [14] Y.-H. Chen, J. T. Daub, F.-K. Guo, B. Kubis, U.-G. Meißner and B.-S. Zou, *Effect of Z_b states on $\Upsilon(3S) \rightarrow \Upsilon(1S)\pi\pi$ decays*, *Phys. Rev.* **D93** (2016) 034030, [[1512.03583](#)].
- [15] V. Baru, J. Haidenbauer, C. Hanhart, A. E. Kudryavtsev and U.-G. Meißner, *Flatte-like distributions and the $a_0(980)/f_0(980)$ mesons*, *Eur. Phys. J. A* **23** (2005) 523, [[nucl-th/0410099](#)].
- [16] M. Cleven, F.-K. Guo, C. Hanhart and U.-G. Meißner, *Bound state nature of the exotic Z_b states*, *Eur. Phys. J. A* **47** (2011) 120, [[1107.0254](#)].
- [17] C. Hanhart, Yu. S. Kalashnikova, P. Matuschek, R. V. Mizuk, A. V. Nefediev and Q. Wang, *Practical Parameterisation for Line Shapes of Near-Threshold States*, *Phys. Rev. Lett.* **115** (2015) 202001, [[1507.00382](#)].
- [18] F. K. Guo, C. Hanhart, Yu. S. Kalashnikova, P. Matuschek, R. V. Mizuk, A. V. Nefediev et al., *Interplay of quark and meson degrees of freedom in near-threshold states: A practical parameterisation for line shapes*, *Phys. Rev.* **D93** (2016) 074031, [[1602.00940](#)].
- [19] M. B. Voloshin, *Radiative transitions from $\Upsilon(5S)$ to molecular bottomonium*, *Phys. Rev.* **D84** (2011) 031502, [[1105.5829](#)].
- [20] T. Mehen and J. W. Powell, *Heavy Quark Symmetry Predictions for Weakly Bound B-Meson Molecules*, *Phys. Rev.* **D84** (2011) 114013, [[1109.3479](#)].
- [21] A. E. Bondar, R. V. Mizuk and M. B. Voloshin, *Bottomonium-like states: Physics case for energy scan above the $B\bar{B}$ threshold at Belle-II*, *Mod. Phys. Lett.* **A32** (2017) 1750025, [[1610.01102](#)].
- [22] V. Baru, E. Epelbaum, A. A. Filin, C. Hanhart, U.-G. Meißner and A. V. Nefediev, *Heavy-quark spin symmetry partners of the $X(3872)$ revisited*, *Phys. Lett.* **B763** (2016) 20–28, [[1605.09649](#)].
- [23] Z.-F. Sun, J. He, X. Liu, Z.-G. Luo and S.-L. Zhu, *$Z_b(10610)^\pm$ and $Z_b(10650)^\pm$ as the $B^*\bar{B}$ and $B^*\bar{B}^*$ molecular states*, *Phys. Rev.* **D84** (2011) 054002, [[1106.2968](#)].
- [24] J. M. Dias, F. Aceti and E. Oset, *Study of $B\bar{B}^*$ and $B^*\bar{B}^*$ interactions in $I = 1$ and relationship to the $Z_b(10610)$, $Z_b(10650)$ states*, *Phys. Rev.* **D91** (2015) 076001, [[1410.1785](#)].
- [25] E. Epelbaum, H.-W. Hammer and U.-G. Meißner, *Modern Theory of Nuclear Forces*, *Rev. Mod. Phys.* **81** (2009) 1773–1825, [[0811.1338](#)].
- [26] S. Fleming, T. Mehen and I. W. Stewart, *NNLO corrections to nucleon-nucleon scattering and perturbative pions*, *Nucl. Phys.* **A677** (2000) 313–366, [[nucl-th/9911001](#)].
- [27] V. Baru, E. Epelbaum, A. A. Filin, C. Hanhart, U.-G. Meißner and A. V. Nefediev, *Quark mass dependence of the $X(3872)$ binding energy*, *Phys. Lett.* **B726** (2013) 537–543, [[1306.4108](#)].
- [28] V. Baru, E. Epelbaum, A. A. Filin, J. Gegelia and A. V. Nefediev, *Binding energy of the $X(3872)$ at unphysical pion masses*, *Phys. Rev.* **D92** (2015) 114016, [[1509.01789](#)].

- [29] M. Jansen, H. W. Hammer and Y. Jia, *Light quark mass dependence of the $X(3872)$ in an effective field theory*, *Phys. Rev.* **D89** (2014) 014033, [[1310.6937](#)].
- [30] V. Baru, A. A. Filin, C. Hanhart, Yu. S. Kalashnikova, A. E. Kudryavtsev and A. V. Nefediev, *Three-body $D\bar{D}\pi$ dynamics for the $X(3872)$* , *Phys. Rev.* **D84** (2011) 074029, [[1108.5644](#)].
- [31] M. Albaladejo, F. K. Guo, C. Hidalgo-Duque, J. Nieves and M. P. Valderrama, *Decay widths of the spin-2 partners of the $X(3872)$* , *Eur. Phys. J.* **C75** (2015) 547, [[1504.00861](#)].
- [32] J. Nieves and M. P. Valderrama, *The Heavy Quark Spin Symmetry Partners of the $X(3872)$* , *Phys. Rev.* **D86** (2012) 056004, [[1204.2790](#)].
- [33] M. T. AlFiky, F. Gabbiani and A. A. Petrov, *$X(3872)$: Hadronic molecules in effective field theory*, *Phys. Lett.* **B640** (2006) 238–245, [[hep-ph/0506141](#)].
- [34] M. P. Valderrama, *Power Counting and Perturbative One Pion Exchange in Heavy Meson Molecules*, *Phys. Rev.* **D85** (2012) 114037, [[1204.2400](#)].
- [35] C. Hidalgo-Duque, J. Nieves, A. Ozpineci and V. Zamiralov, *$X(3872)$ and its Partners in the Heavy Quark Limit of QCD*, *Phys. Lett.* **B727** (2013) 432–437, [[1305.4487](#)].
- [36] C. Hidalgo-Duque, J. Nieves and M. P. Valderrama, *Light flavor and heavy quark spin symmetry in heavy meson molecules*, *Phys. Rev.* **D87** (2013) 076006, [[1210.5431](#)].
- [37] J. Hu and T. Mehen, *Chiral Lagrangian with heavy quark-diquark symmetry*, *Phys. Rev.* **D73** (2006) 054003, [[hep-ph/0511321](#)].
- [38] S. Fleming, M. Kusunoki, T. Mehen and U. van Kolck, *Pion interactions in the $X(3872)$* , *Phys. Rev.* **D76** (2007) 034006, [[hep-ph/0703168](#)].
- [39] ALPHA collaboration, F. Bernardoni, J. Bulava, M. Donnellan and R. Sommer, *Precision lattice QCD computation of the $B^*B\pi$ coupling*, *Phys. Lett.* **B740** (2015) 278–284, [[1404.6951](#)].
- [40] J. Nieves and M. P. Valderrama, *Deriving the existence of $B\bar{B}^*$ bound states from the $X(3872)$ and Heavy Quark Symmetry*, *Phys. Rev.* **D84** (2011) 056015, [[1106.0600](#)].
- [41] B. Grinstein, E. E. Jenkins, A. V. Manohar, M. J. Savage and M. B. Wise, *Chiral perturbation theory for f_{D_s}/f_D and B_{B_s}/B_B* , *Nucl. Phys.* **B380** (1992) 369–376, [[hep-ph/9204207](#)].
- [42] V. Baru, E. Epelbaum, A. A. Filin, C. Hanhart and A. V. Nefediev, *Molecular partners of the $X(3872)$ from heavy-quark spin symmetry: a fresh look*, *EPJ Web Conf.* **137** (2017) 06002.
- [43] V. Baru, C. Hanhart, A. E. Kudryavtsev and U.-G. Meißner, *The Role of the nucleon recoil in low-energy meson nucleus reactions*, *Phys. Lett.* **B589** (2004) 118–124, [[nucl-th/0402027](#)].
- [44] V. Baru, E. Epelbaum and A. Rusetsky, *The Role of nucleon recoil in low-energy antikaon-deuteron scattering*, *Eur. Phys. J.* **A42** (2009) 111–120, [[0905.4249](#)].
- [45] M. B. Voloshin, *Modification by pion exchange of near threshold resonance line shape in open heavy flavor channel*, *Phys. Rev.* **D92** (2015) 114003, [[1507.02639](#)].